López-Lanuza, G., Chen-Hu, K., & Armada, A. G. (10-13 April 2022). *Deep Learning-Based Optimization for Reconfigurable Intelligent Surface-Assisted Communications* [proceedings]. 2022 IEEE Wireless Communications and Networking Conference (WCNC), Austin, USA.

DOI: 10.1109/wcnc51071.2022.9771876

Deep Learning-Based Optimization for Reconfigurable Intelligent Surface-Assisted Communications

Guillermo López-Lanuza, Kun Chen-Hu and Ana García Armada
Deparment of Signal Theory and Communications, Universidad Carlos III de Madrid, Spain
E-mails: {glopez, kchen, agarcia}@tsc.uc3m.es

***Abstract*—Reconfigurable Intelligent Surfaces (RISs) are an emerging technology in the evolution towards the Sixth Generation (6G) of mobile communications. They are capable of enhancing the overall system performance and extending the coverage of the existing cells. They are built by a large amount of low-cost meta-elements that can be configured by tuning their phase shifts, and hence, the channel response can be constructively combined and forwarded to some specific direction. Many algorithms have been proposed to obtain the optimum phase shifts, generally assuming a single-carrier system and/or a medium-size RIS to constrain the complexity of the optimization process. In this work, we propose a flexible and scalable unsupervised learning model, capable of obtaining the best phase shifts for any scenario. Our proposal is able to handle multi-carrier waveforms and very large-size RIS, considering both continuous and discrete phase shifts. Besides, we also propose the use of clustering to reduce further the complexity while maintaining the performance. A comparison in terms of achievable rate and time execution is provided in order to show the superiority of our proposal against the existing solutions.**

I. Introduction

The Fifth and Sixth Generation (5G and 6G) of mobile communication systems will exploit the frequencies between $30-300$ GHz, typically known as millimetre waves (mm-Wave) [1], to leverage the greater available bandwidth. Nonetheless, one of the main drawbacks of these high frequencies is the strong path-loss due to the atmospheric absorption. Several techniques have been proposed to face it. Massive Multiple Input Multiple Output (mMIMO) [2] is a well-known technique, where a large number of antenna elements deployed at the base station (BS) are exploited to focus the energy towards the user equipment (UE), and hence compensate the path-loss. Commonly, this technique is known as active beamforming [3], [4]. An alternative way to circumvent this issue consists in deploying relays between the BS and UEs [5], based on techniques such as Amplify-and-Forward [6] or Decode-and-Forward [7]. All these schemes enhance the performance of the communication link at the expense of significantly increasing the cost and the energy consumption of the network.

Reconfigurable Intelligent Surfaces (RISs) [8], [9] have been recently proposed to either improve the performance of the cell or extend the coverage to those areas with a difficult access. These surfaces are built by low-cost meta-materials [10], which are able to modify and forward the received radio waves to any direction [11], avoiding the use of expensive radio-frequency chains. The reconfigurability can be enabled by adjusting the phase shifts introduced by each passive reflecting element of the RIS. Therefore, the signals after channel propagation can be constructively aligned, incrementing the Signal-to-Interference and Noise Ratio (SINR), without increasing the overall hardware and energy cost [12].

The key to obtain a good performance in RIS-assisted communication systems is the joint design of the MIMO pre/post-coding at the transmit and receive ends and the phase shifts of the surface [13], [14], [15], [16]. However, the optimization problem becomes non-convex, and typically, sub-optimal solutions are provided at the expense of sacrificing the performance, or constraining the dimension of the optimization by circumscribing them to low-size surfaces and single-carrier waveforms. On the other hand, several works focus on channel estimation [17], [18], showing that RIS-assisted links require a significant amount of reference signals in order to obtain the cascaded channel estimates (product of the channel between the BS-RIS and RIS-UE), whose accuracy has a significant impact in the performance of the system. Moreover, the phase configuration of the RIS is typically quantized by a finite number of bits to avoid higher cost and complexity in the manufacturing process [19].

Recently, Neural Networks (NNs) [20], [21] have been exploited to solve the complex optimization problems associated to the RIS-empowered scenarios. Reference [22] proposed a supervised learning approach to design the optimal RIS configuration. However, the main downside of supervised methods is the difficulty of collecting samples and building a dataset to train the model, which is unfeasible in realistic scenarios. Lately, [23] proposed an unsupervised learning method to obtain the optimal phase shifts, achieving almost the same performance as [13] with a significant reduction of the complexity. Nevertheless, it is constrained to single-carrier waveforms and low-size RIS.

In this paper, we propose a new technique to obtain the phase shifts of the RIS by exploiting deep learning based on an unsupervised model, similar to [23]. However, our method is specially designed and accordingly scaled for large-size RIS and broadband waveforms, also considering discrete phase shifts. Additionally, in order to reduce the complexity further, clustering is also proposed so as to classify the passive reflecting elements in several groups according to their cascaded channel estimates at all subcarriers, and then, the NN is executed to configure the same phase shift for all the elements in the same group. In order to show the performance of our proposal, we provide comparison in terms of achievable rates

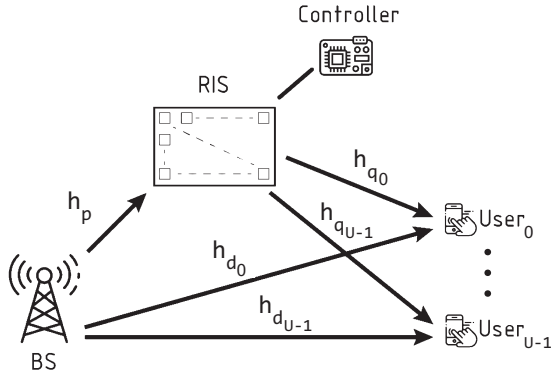

Figure 1: System model of the RIS-assisted communication link.

(bits per second) and complexity (required time execution) for the different methods. The results will show that our proposal is efficient in the design of the phase shifts of RIS elements.

The upcoming sections of this paper are organized as follows: in Section II, the proposed system, channel model, channel estimation and problem formulation are addressed. Section III presents the proposed optimization using NNs. The experiments carried out and the results obtained are shown in Section IV, and conclusions are given in Section V.

II. System Model

We consider a system consisting of a BS equipped with a single transmit antenna, a RIS with M passive reflecting elements and U UEs equipped with a single receiver antenna each[1]. Despite the fact that the BS could be equipped with more than one antenna, hence enhancing the performance, a system similar to the one in [15], [17] is considered. A controller is connected to the RIS to adjust the phase shifts (see Fig. 1). Orthogonal Frequency Division Multiplexing (OFDM) [24] is the chosen waveform, whose number of subcarriers is K, and we assume that the length of the cyclic prefix is long enough to absorb the multi-path effects of the channel. Additionally, for simplicity we assume that Time Division Multiple Access (TDMA) is deployed, where all UEs are multiplexed in different OFDM symbols. This will allow us to optimize the RIS for each user in different time slots[2].

Therefore, from now on we center on the signal that is transmitted from the BS to any given UE, made up of N consecutive OFDM symbols. The baseband received signal at the UE at k-th subcarrier and n-th OFDM symbol $y_{_{k,n}} \in \mathbb{C}$ is given by

$$y_{_{k,n}} = h_{\theta_{_{k,n}}} x_{_{k,n}} + n_{_{k,n}} = (h_{d_{k,n}} + h_{r_{_{k,n}}}) x_{_{k,n}} + n_{_{k,n}}, \quad (1)$$
$$k = 0, \ldots, K-1, \quad n = 0, \ldots, N-1,$$

where $h_{\theta_{_{k,n}}} \in \mathbb{C}$ is the equivalent channel between the BS and the UE at the k-th subcarrier and n-th OFDM symbol, which is composed by the addition of the direct and reflected channels ($h_{d_{k,n}} \in \mathbb{C}$ and $h_{r_{_{k,n}}} \in \mathbb{C}$, respectively), $x_{k,n} \in \mathbb{C}$ denotes the data symbol to be sent to the UE at the k-th subcarrier and n-th OFDM symbol, and $n_{k,n} \in \mathbb{C}$ is the complex additive white Gaussian noise (AWGN) distributed as $\mathcal{CN}\left(0, \sigma_n^2\right)$.

According to Fig. 1, the RIS-aided channel h_r in (1) can be decomposed as

$$h_{r_{_{k,n}}} = \sum_{m=0}^{M-1} h_{c_{_{k,n,m}}} e^{j\theta_{_{n,m}}} = \sum_{m=0}^{M-1} h_{p_{_{k,n,m}}} h_{q_{_{k,n,m}}} e^{j\theta_{_{n,m}}}, \quad (2)$$
$$k = 0, \ldots, K-1, \quad n = 0, \ldots, N-1,$$

where $h_{c_{_{k,n,m}}}$ is the cascaded channel between the BS and the UE for the m-th passive element of the RIS at k-th subcarrier and n-th OFDM symbol, which is a product of the channel between BS-RIS and RIS-UE ($h_{p_{_{k,n,m}}} \in \mathbb{C}$ and $h_{q_{_{k,n,m}}} \in \mathbb{C}$, respectively), and $\theta_{_{n,m}} \in [-\pi, \pi)$ corresponds to the phase shift of the m-th RIS element at n-th OFDM symbol.

A. Channel model

We assume that the channel remains quasi-static during the transmission of N consecutive OFDM symbols to a given UE. Hence, for simplicity we drop the subindex n for the channel coefficients given in (1) and (2).

Regarding the channel model, the geometry-based clustered delay line (CDL) is considered, which is proposed in the 5G standard [25] for system level evaluation. For a particular path indexed by l, the multi-path channel response in the time domain between the RIS and the UE is given by

$$\tilde{h}_{q_{l,m}} = \sqrt{\beta_{q_l}} a_{q_l} f_{x,y}(\phi_{q_{l,m}}, \vartheta_{q_{l,m}}) \delta\left[\tau - l\right], \quad (3)$$
$$l = 0, \ldots, L_q - 1,$$
$$x = 0, \ldots, M_x - 1, \quad y = 0, \ldots, M_y - 1, \quad m = xM_y + y,$$

where $\delta(\bullet)$ is the Dirac delta function, τ is the time delay measured in samples, L_q is the length of the channel in samples, β_{q_l} and a_{q_l} correspond to the path-loss and small scale fading coefficient, respectively, for l-th scatterer, $\phi_{q_{l,m}}$ and $\vartheta_{q_{l,m}}$ are the azimuth and elevation angles, respectively, of the l-th tap, and $f_{x,y}$ denotes the steering vector. Assuming that the RIS is a rectangular array ($M = M_x M_y$), the steering vector can be expressed [26] as

$$f_{x,y}(\phi, \vartheta) = e^{jxkd_x sin\vartheta cos\phi} e^{jykd_y sin\vartheta sin\phi}, \quad (4)$$
$$x = 0, \ldots, M_x - 1, \quad y = 0, \ldots, M_y - 1, \quad k = 2\pi/\lambda,$$

being λ the wavelength, and d_x and d_y corresponding to the distances between any two contiguous adjacent elements in the x-axis and y-axis, respectively.

Analogously to the channel in the direction RIS-UE, the multi-path channel response in the time domain for the l-th path between the BS and the RIS is given by

$$\tilde{h}_{p_{l,m}} = \sqrt{\beta_{p_l}} a_{p_l} f_{x,y}(\phi_{p_{l,m}}, \vartheta_{p_{l,m}}) \delta\left[\tau - l\right], \quad (5)$$
$$l = 0, \ldots, L_p - 1,$$

[1]For ease of exposition we focus on the downlink, but the same approach is completely applicable to the uplink.

[2]Allocating different subcarriers to different users would change the notation but not substantially the problem formulation and solution.

$$x = 0, \ldots, M_x - 1, \quad y = 0, \ldots, M_y - 1, \quad m = xM_y + y,$$

where L_p is the length of the channel in samples.

The frequency-domain channel response given in (2) can be obtained by applying the Discrete Fourier Transform (DFT) [27] to (3) and (5) as

$$h_{q_{k,m}} = \frac{1}{\sqrt{K}} \sum_{l=0}^{L_q-1} \tilde{h}_{q_{l,m}} e^{-j2\pi \frac{kl}{K}}, \quad k = 0, \ldots, K-1, \quad (6)$$

$$h_{p_{k,m}} = \frac{1}{\sqrt{K}} \sum_{l=0}^{L_p-1} \tilde{h}_{p_{l,m}} e^{-j2\pi \frac{kl}{K}}, \quad k = 0, \ldots, K-1, \quad (7)$$

respectively.

B. Channel estimation

In order to obtain the channel estimates for the UE, N_p OFDM symbols out of N are exclusively adopted for the transmission of the reference signals. Then, $N - N_p$ OFDM symbols are used for data transmission [17], [18].

The channel estimates are obtained using the Least Squares (LS) technique [28], which is given by

$$\widehat{h}_{\theta_k} = \frac{y_{k,n}}{\dot{x}_{k,n}} = \widehat{h}_{d_k} + \sum_{m=0}^{M-1} \widehat{h}_{c_{k,m}} e^{j\dot{\theta}_{n,m}} + n'_{k,n}, \quad (8)$$

where $\dot{x}_{k,n}$ denotes the pilot symbol at k-th subcarrier and n-th OFDM symbol ($0 \leq n \leq N_p - 1$), $\dot{\theta}_{n,m}$ accounts for the phase shift configured in the m-th RIS element at n-th OFDM symbol (which are known at this training stage), and $\widehat{h}_{d_k}$, $\widehat{h}_{c_{k,m}}$ are the estimates of the direct and cascaded channels, respectively, at k-th subcarrier for the m-th RIS element.

Inspecting (8) and according to [17], [18], these estimates can be obtained by transmitting $N_p = M + 1$ pilot symbols from the BS to the UE, and hence, the channel estimation can be obtained by solving a system of linear equations.

However, the estimation is polluted by noise, which can be harmful in the computation of the phase shifts. In order to reduce this error, the time responses of the estimated cascaded channel for each passive element are computed, and only the $L_p + L_q - 1$ strongest values are kept, similarly to [29]. Furthermore, the highest energy taps above an energy threshold can be chosen as proposed in [30]. Hence, for the purpose of channel estimation, the reduced noise variance can be upper-bounded as

$$\sigma_{\tilde{n}}^2 \leq \frac{L_p + L_q - 1}{K} \sigma_n^2, \quad (9)$$

where typically the number of subcarriers is always much higher than the number of taps of the channel response.

C. Problem formulation

Assuming that the channel estimation error is negligible thanks to the de-noising procedure previously explained, the performance of the RIS-empowered link is characterized by the achievable rate of the UE as

$$R\,[\text{bps}] = B \sum_{k=0}^{K-1} \log_2 \left(1 + \frac{P}{\sigma_n^2} |h_{\theta_k}|^2\right), \quad (10)$$

where B denotes the bandwidth and P is the transmit power allocated per subcarrier. For simplicity, we consider constant power allocation in all K subcarriers following [31] proposal, and we also assume that the signals of all U UEs are being transmitted with the same power per subcarrier P. Therefore, due to the use of TDMA, the rate for each UE can be independently maximized as

$$\max_{\theta_m} \sum_{k=0}^{K-1} \log_2 \left(1 + \frac{P}{\sigma_n^2} \left| h_{d_k} + \sum_{m=0}^{M-1} h_{c_{k,m}} e^{j\theta_m} \right|^2\right), \quad (11)$$
$$\text{s.t.} \quad \theta_m \in [-\pi, \pi), \quad m = 0, \ldots, M-1.$$

Besides, to provide a more realistic case, the values of the phase shifts in (11) can be also restricted to a discrete set,

$$\theta_m \in \frac{2\pi}{2^b} \left\{0, 1, \ldots, 2^b - 1\right\}, \quad (12)$$

where b is the available number of bits for controlling the phase shifts of RIS elements. Therefore, we name these scenarios as continuous and discrete phase shifts cases, respectively.

III. Neural Network Optimization for RIS-aided communication

The nature of the problem given in (11) is non-convex due to the shape of the objective function to be maximized, as pointed out in [13]. Moreover, when discrete phase shifts as in (12) are considered, its complexity is even higher [14].

Therefore, a NN is exploited in order to circumvent this complexity and maintain the performance, as explained further in Section I and similarly to the works of [20], [21], [22], [23], where the proposed optimization technique is based on a deep learning model which is able to find the best set of θ_m for each UE to maximize the achievable rate. Furthermore, it is trained in an unsupervised way, making our approach more suitable than supervised techniques due to the fact that the data gathering, labelling and training procedures are not required. Note that our proposal is feasible for multi-carrier waveform as well as very large number of passive elements of the RIS, unlike [23]. Furthermore, a clustering algorithm is considered to be applied firstly in order to group RIS elements and decrease even further the complexity of the problem.

A. Clustering

Due to the spatial correlation present in the RIS array, the large number of passive elements and the high amount of subcarriers in the OFDM, many of these reflecting elements may face the same, or very similar, cascaded channel coefficients. Consequently, the RIS elements can be grouped into different clusters according to their estimated cascaded channel coefficient $\widehat{h}_{c_{k,m}}$, producing M_g subpanels whose elements are configured with the same phase shift value [11] in order to reduce the hardware/software complexity and speed up the processing. For this work at issue K-Means [32] is chosen, where each RIS element gets represented by a vector of K components in order to be clustered.

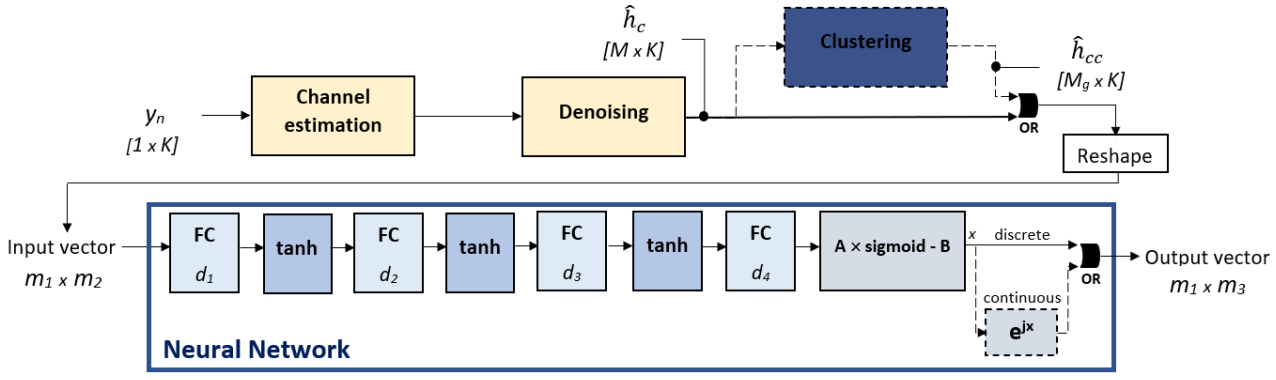

Figure 2: Block diagram of the proposed technique based on channel estimation, preprocessing and unsupervised learning. The dashed line blocks mean that they are optional, depending on the scenario. The gates represent OR logical gates.

B. Neural Network

The proposed network is shown in Fig. 2, where FC denotes a fully-connected layer, $tanh$ is the hyperbolic tangent function, $sigmoid$ is the sigmoid function, and the last block is an optional customizable layer defined as e^{jx}, being x the input. The dimensions of the input and output vectors of the NN (m_1, m_2 and m_3) are determined by the size of the cascaded channel estimates, and are given by

$$\{m_1, m_2, m_3\} = \begin{cases} \{M_g, 2K, 1\}, & K > 1 \\ \{1, 2M_g, M_g\}, & K = 1, \end{cases} \tag{13}$$

where the factor 2 is due to the concatenation of the real and imaginary parts of the complex cascaded channel estimates. Note that if clustering is not carried out, $M_g = M$.

Regarding hidden layers, their dimensions are proportional to the input dimensions so as to obtain a higher flexibility (wide range of values for m_1 and m_2) and guarantee the network learning ability with system scaling, hence they are set to

$$\{d_1, d_2\} = \begin{cases} m_2 + \{m_1/2, m_1\}, & K > 1, m_1 < 2m_2 \\ \{m_1/2, m_1\}, & K > 1, m_1 \geq 2m_2 \\ \{2m_2, 4m_2\}, & K = 1 \end{cases} \tag{14}$$

$$d_3 = m_2, \quad d_4 = m_3.$$

In our proposal, the number of hidden layers and the scaling factors in hidden dimensions with respect to m_1, m_2 have been chosen to achieve a trade-off between performance and cost.

Hyperbolic tangent is chosen as the activation function to be used between hidden layers, and a sigmoid layer multiplied by a coefficient A with an offset $-B$ is implemented as the final activation layer, where A and B values depend on hardware constraints regarding phase shifts in study cases as

$$\{A, B\} = \begin{cases} \{2\pi, \pi\}, & \theta_m \in [-\pi, \pi) \\ \{2, 1\}, & \theta_m \in \{0, \pi\}. \end{cases} \tag{15}$$

Note that with continuous phase shifts, the output of the NN is the phase configuration θ_m, hence and additional layer is required to obtain the reflection coefficient $e^{j\theta_m}$. On the contrary, for the case of discrete phase shifts, the output of the NN is already $e^{j\theta_m}$. Additionally, for the case of discrete phase shifts, the results provided by the NN are required to be rounded to the discrete set of values to fulfill hardware requirements.

IV. Experiments and Results

A. Experiments

In this section, numerical results in terms of achievable rates and execution times are shown to compare our proposal to existing solutions.

Data are obtained from *IEEE Signal Processing Cup 2021: Configuring an Intelligent Reflecting Surface for Wireless Communications*[3]. These data encompass the pilot transmit signals $\dot{x}$ for U = 50 users, their corresponding receive signals y and the phase shifts $\dot{\theta}$ used in pilots transmission. Moreover, the maximum number of taps is set to $L_p + L_q - 1 = 20$, the number of subcarriers is $K = 500$, the bandwidth is $B = 10$ MHz and the RIS is composed of $M = 4096$ meta-elements.

As for spatial distribution, the links between the BS and RIS have Line-Of-Sight (LOS) while some of the RIS-UE links are LOS and some others are Non-LOS (NLOS). In particular, 36 UEs have LOS with the RIS and the rest 14 UEs do not. Direct path between the BS and the UEs is NLOS for all UEs.

Regarding the channel estimation stage, similarly to [17], the phase shifts of the RIS during the transmission of the pilot symbols are set using a Hadamard matrix of order N_p [33].

The experiments are performed using *PyTorch* framework with Adam optimizer and a learning rate equal to 10^{-4}. The number of iterations are set to 100 and 50 for the continuous and discrete cases, respectively. Furthermore, in order to avoid potential local maximum points, each optimization has been performed by exploiting 5 different initializations. All of them were run in an Intel i7-8565U CPU @ 1.80 GHz (8 CPUs).

B. Performance comparison to the state-of-the-art

In this section, an achievable rate comparison is provided so as to show the performance of our proposal. In order to be able to compare our work to the one of [23], we must particularize our proposal to the scenario imposed by [23]. Therefore, the system is constrained to use a single-carrier waveform ($K = 1$), the phase shifts correspond to the continuous case and the size of the RIS is reduced to $M = 64$.

[3]Available at https://kth.box.com/v/spcup2021-dataset2

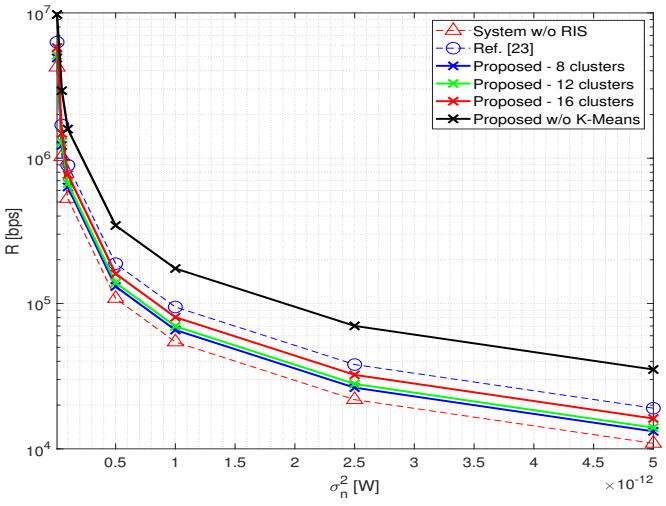

Figure 3: Average achievable rate for $M = 64$, $K = 1$ and $\theta \in [-\pi, \pi)$.

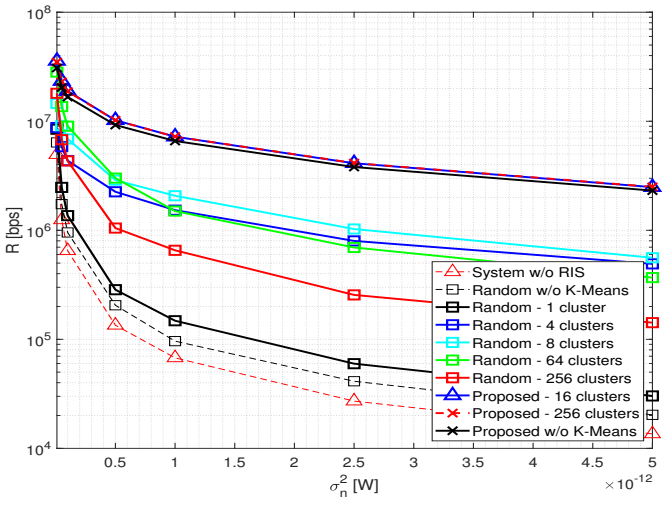

Figure 4: Average achievable rate for $M = 4096$, $K = 500$ and $\theta \in \{0, \pi\}$.

Fig. 3 shows the average achievable rate for all UEs for different noise powers σ_n^2 assuming $P = 1$ W. Note that, as defined in (3) and (5), the path-loss term is incorporated in the channels, ranging from $6.55 \cdot 10^{-12}$ to $7.65 \cdot 10^{-13}$ for h_d and from $9.62 \cdot 10^{-16}$ to $9.35 \cdot 10^{-18}$ for h_c within the U users. It can be observed that our proposal without clustering clearly outperforms the approach of [23], which is shown to perform very close to the traditional semi-definite relaxation (SDR) technique [13]. When clustering is applied (with 8, 12 and 16 clusters), the performance is slightly worse than for the reference case since there is neither too much spatial nor frequency correlation to be exploited in such a simple scenario. However, as we show in Section IV-D, the execution time is significantly reduced.

C. Performance comparison in realistic scenarios

In this section, we focus on a scenario with a multi-carrier waveform (K = 500) and a large amount of RIS elements (M = 4096) in which state-of-the-art literature is not able to work because of its complexity. With the aim to provide a reference case, we also evaluate the performance of a baseline random phase configuration, which consists in sampling random values from the set of possible phase shifts.

Table 1: Execution time of different algorithms.

Algorithm			**Execution time (iteration time)**
M = 64 **K = 1** $\theta \in$ **[-π, π)**	Ref. [23]		1130.96 s (45.23 ms)
	Proposed	8 clusters	157.52 s (6.30 ms)
		12 clusters	166.57 s (6.66 ms)
		16 clusters	169.78 s (6.79 ms)
		w/o K-Means	180.23 s (7.21 ms)
M = 4096 **K = 500** $\theta \in$ **{0, π}**	Random	1 cluster	0.01 s
		4 clusters	43.48 s
		8 clusters	68.91 s
		64 clusters	220.81 s
		256 clusters	820.35 s
		w/o K-Means	2.75 s
	Proposed	16 clusters	586.18 s (39.19 ms)
		256 clusters	1884.78 s (85.31 ms)
		w/o K-Means	6916.04 s (553.28 ms)

Fig. 4 provides an achievable rate comparison for this realistic scenario considering discrete phase shifts, more specifically a single bit. We can see that our proposal significantly improves the performance as compared to the random case. We can also see that clustering is helping to improve the performance for both cases, showing that the spatial correlation is relevant in the overall performance for large-size RIS and broadband signals. Regarding our proposal, clustering reduces the complexity of the optimization problem by decreasing the dimensionality of it, and hence, the results easily converge. Therefore, it is specially interesting and advantageous in complex scenarios with a large number of both RIS elements and subcarriers, where strong correlation is shown in both spatial and frequency domains, in contrast to simpler scenarios like the one in Section IV-B. In order to improve the performance of the proposed technique without clustering, more iterations are required at the expense of sacrificing hardware resources and time execution, which is not recommendable, if at all feasible, for realistic communication scenarios.

D. Execution time comparison

In real-time communications, specially for low-latency ones, the execution time is as important as the performance due to the fact that an increment of the delay may negatively affect many services. Table 1 describes the overall required execution time in seconds (s) and mili-seconds (ms) representing the computational cost of each scenario and algorithm. Time on the experiment of random phase shifts accounts for performing K-Means, sampling M_g times from $\{0, \pi\}$ and reassigning sampled values to the M elements following clustering results. As for the time of the work of [23], it only includes NN optimization, while the time of our proposal includes clustering, NN optimization and reassignment of phase shifts according to K-Means results. We can see that our proposal is not only outperforming [23], but it is also more than six times faster. Besides, [23] is proved to greatly reduce the time consumption

of SDR algorithm [13]. On the other hand, we can see that using random phases lead to the best execution time since it does not require an additional optimization. However, the achievable rate of our proposal is significantly higher. Additionally, we can see that clustering meaningfully reduces the execution time, facilitating the optimization process and still achieving a substantial performance gain.

V. Conclusions

In this work we propose a realistic optimization technique for RIS-aided communications, based on unsupervised deep learning in order to deal with the great complexity associated to RIS-assisted systems. The proposal can be easily exploited for broadband waveforms, large-size RIS and discrete phase shifts, not as other previous contributions, making it suitable for low-cost passive reflecting elements. Our proposal outperforms the state-of-the-art techniques and avoids an increase in the complexity. Additionally, clustering is also able to reduce the execution time even further with a performance loss that is in some cases negligible, where the optimum number of clusters depends on the signal-to-noise ratio and the scenario itself, and which is specially interesting in lifelike environments with strong spatial and frequency correlation. Consequently, our proposal enables the RIS to be exploited for high performance links with feasible complexity and execution times.

Acknowledgment

This work has been funded by the Spanish National projects IRENE-EARTH (PID2020-115323RB-C33 / AEI / 10.13039/501100011033) and AMATISTA (CDTI IDI-20200861).

References

[1] "New frequency range for NR (24.25-29.5 GHz) (Release 15)," 3GPP, France, Technical Report 38.815, Jun. 2018.

[2] F. W. Vook, T. A. Thomas, and E. Visotsky, "Massive mimo for mmwave systems," in *2014 48th Asilomar Conference on Signals, Systems and Computers*, Nov 2014, pp. 820–824.

[3] S. Kutty and D. Sen, "Beamforming for millimeter wave communications: An inclusive survey," *IEEE Communications Surveys Tutorials*, vol. 18, no. 2, pp. 949–973, 2016.

[4] T. Engda, Y. Wondie, and J. Steinbrunn, "Massive mimo, mmwave and mmwave-massive mimo communications: Performance assessment with beamforming techniques," Sep. 2020.

[5] K. Ntontin, M. Renzo, J. Song, F. Lazarakis, J. Rosny, D.-T. Phan-Huy, O. Simeone, R. Zhang, M. Debbah, G. Lerosey, M. Fink, S. Tretyakov, and S. Shamai, "Reconfigurable intelligent surfaces vs. relaying: Differences, similarities, and performance comparison," 08 2019.

[6] L. J. Rodriguez, N. Tran, and T. Le-Ngoc, *Amplify-and-Forward Relaying in Wireless Communications*. Springer International Publishing, 2015.

[7] E. M. a. Elsheikh, *Wireless Decode-And-Forward Relay Channels*. LAP Lambert Academic Publishing, 2010.

[8] Q. Wu and R. Zhang, "Intelligent reflecting surface enhanced wireless network via joint active and passive beamforming," *IEEE Transactions on Wireless Communications*, vol. 18, no. 11, pp. 5394–5409, Nov 2019.

[9] M. Siddiqi, T. Mir, M. Hao, and R. MacKenzie, "Low-complexity joint active and passive beamforming for ris-aided mimo systems," *Electronics Letters*, Mar. 2021.

[10] Q. Wu and R. Zhang, "Towards smart and reconfigurable environment: Intelligent reflecting surface aided wireless network," *IEEE Communications Magazine*, vol. 58, no. 1, pp. 106–112, Jan. 2020.

[11] E. Björnson, H. Wymeersch, B. Matthiesen, P. Popovski, L. Sanguinetti, and E. de Carvalho, "Reconfigurable intelligent surfaces: A signal processing perspective with wireless applications," Feb. 2021.

[12] Q. Wu and R. Zhang, "Beamforming optimization for intelligent reflecting surface with discrete phase shifts," in *ICASSP 2019 - 2019 IEEE International Conference on Acoustics, Speech and Signal Processing (ICASSP)*, May 2019, pp. 7830–7833.

[13] Q. Wu and R. Zhang, "Intelligent reflecting surface enhanced wireless network: Joint active and passive beamforming design," 2018.

[14] H. Chongwen, A. Zappone, G. Alexandropoulos, m. Debbah, and C. Yuen, "Reconfigurable intelligent surfaces for energy efficiency in wireless communication," *IEEE Transactions on Wireless Communications*, vol. PP, pp. 1–1, Jun. 2019.

[15] Y. Yang, B. Zheng, S. Zhang, and R. Zhang, "Intelligent reflecting surface meets ofdm: Protocol design and rate maximization," *IEEE Transactions on Communications*, vol. PP, pp. 1–1, Mar. 2020.

[16] Y. Cao, T. Lv, and W. Ni, "Intelligent reflecting surface aided multi-user millimeter-wave communications for coverage enhancement," Oct. 2019.

[17] C. You, B. Zheng, and R. Zhang, "Channel estimation and passive beamforming for intelligent reflecting surface: Discrete phase shift and progressive refinement," *IEEE Journal on Selected Areas in Communications*, vol. 38, no. 11, pp. 2604–2620, Nov. 2020.

[18] Z.-Q. He and X. Yuan, "Cascaded channel estimation for large intelligent metasurface assisted massive mimo," *IEEE Wireless Communications Letters*, vol. 9, no. 2, pp. 210–214, 2020.

[19] Y. Han, W. Tang, S. Jin, C. Wen, and X. Ma, "Large intelligent surface-assisted wireless communication exploiting statistical csi," *IEEE Transactions on Vehicular Technology*, vol. PP, pp. 1–1, Jun. 2019.

[20] T. Lin and Y. Zhu, "Beamforming design for large-scale antenna arrays using deep learning," *IEEE Wireless Communications Letters*, vol. PP, pp. 1–1, Sep. 2019.

[21] G. Aceto, A. Montieri, A. Pescapè, and D. Ciuonzo, "Mobile encrypted traffic classification using deep learning: Experimental evaluation, lessons learned, and challenges," *IEEE Transactions on Network and Service Management*, vol. PP, Feb. 2019.

[22] H. Chongwen, G. Alexandropoulos, C. Yuen, and m. Debbah, "Indoor signal focusing with deep learning designed reconfigurable intelligent surfaces," Jul. 2019, pp. 1–5.

[23] J. Gao, C. Zhong, X. Chen, H. Lin, and Z. Zhang, "Unsupervised learning for passive beamforming," *IEEE Communications Letters*, vol. 24, no. 5, pp. 1052–1056, May 2020.

[24] R. W. Chang, "Synthesis of band-limited orthogonal signals for multichannel data transmission," *The Bell System Technical Journal*, vol. 45, no. 10, pp. 1775–1796, Dec. 1966.

[25] "Study on channel model for frequencies from 0.5 to 100 GHz (Release 16)," 3GPP, France, Technical Report 38.901, Dec. 2019.

[26] C. A. Balanis, *Antenna Theory: Analysis and Design*. USA: Wiley-Interscience, 2005.

[27] D. Sundararajan, *The Discrete Fourier Transform: Theory, Algorithms and Applications*. World Scientific Publishing Co Pte Ltd, May 2001.

[28] J.-C. Lin, "Least-squares channel estimation for mobile ofdm communication on time-varying frequency-selective fading channels," *IEEE Transactions on Vehicular Technology*, vol. 57, no. 6, pp. 3538–3550, 2008.

[29] H. Zamiri-Jafarian, M. Omidi, and S. Pasupathy, "Improved channel estimation using noise reduction for ofdm systems," in *The 57th IEEE Semiannual Vehicular Technology Conference, 2003. VTC 2003-Spring.*, vol. 2, 2003, pp. 1308–1312 vol.2.

[30] N. Letzepis, A. Grant, P. Alexander, and D. Haley, "Multipath parameter estimation from ofdm signals in mobile channels," Nov. 2010.

[31] A. Armada, "A simple multiuser bit loading algorithm for multicarrier wlan," in *ICC 2001. IEEE International Conference on Communications. Conference Record (Cat. No.01CH37240)*, 2001, pp. 1168–1171 vol.4.

[32] J. Macqueen, "Some methods for classification and analysis of multivariate observations," in *In 5-th Berkeley Symposium on Mathematical Statistics and Probability*, 1967, pp. 281–297.

[33] A. Hedayat and W. Wallis, "Hadamard matrices and their applications," *The Annals of Statistics*, vol. 6, Nov. 1978.